Position Ground Truth For a Round Robot Using LiDARs

1st João Victor Lourenço Aguiar
Department of Electrical Engineering
Centro Universitário FEI
São Bernardo do Campo, Brazil
0009-0009-2544-0161

2nd Flavio Tonidandel
Department of Computer Science
Centro Universitário FEI
São Bernardo do Campo, Brazil
0000-0003-0345-668X

***Abstract*—Localization is an essential role a robot must have, as it must be autonomous and require less human intervention when operating in society. When developing and testing a localization system, it's crucial to compare what it calculates with a ground truth provided by a sensor not being used in the system developed. Thus, this paper proposes a ground truth approach using two LiDARs to detect with reasonable accuracy the actual position of round robots in the real world, like the ones used in the Small Size League of RoboCup. The league is a considerable scenario for tests since it uses a particular camera system positioned above the field to detect the robot's position, and the internal sensors, like encoders, cannot provide high accuracy due to wheel slipage. The software architecture includes a scan matching step to combine LiDARs, and the detection step is made through the Hough transform to recognize circular patterns in the image created with the LiDAR points. The results showed that the system based on the LiDARs is significant as ground truth, with a mean error of less than 1 centimeter in the 17 positions analyzed in tests and a standard deviation of around 1 centimeter. The results are notable when compared with the league's camera system in these scenarios. The system can be adapted to different sizes of robots and be used in any indoor environment, although the Small Size League was the main scenario for the tests.**

***Index Terms*—Ground Truth, Position, LiDAR, Round Robots.**

I. Introduction

The fast development of technology has ushered in a new era of automation, in which robots are playing a pivotal role in changing industries and the everyday lives of people in several sectors, such as healthcare, manufacturing, agriculture, and even personal assistance. The increase in the use of robots requires more autonomy from them, with the ability to operate less with human intervention and control, such as moving and reaching a goal in an environment, but also more safety when interacting with people.

Localization is an important role that a robot must have to work autonomously in an environment and is a substantial research topic in the robotics field [3], [5], [16]. It's crucial to compare the estimation calculated by these to a ground truth, i.e., the factual localization of the robot in an environment, to evaluate different localization systems [14]. Besides that, using a reliable ground truth is essential to calibrate a localization system being developed, such as a sensor fusion used for robots localization for indoor environments, where using a GPS for ground truth cannot be considered, for example.

RoboCup is an organization with a long-term goal to have a team of humanoid autonomous robots by the middle of the 21st century that will play against the winner of the Human World Cup. This goal has been proposed with the idea of improving and promoting research in robotics [18]. The Small Size League (SSL) is one of the oldest leagues of RoboCup and aims to solve the problem of intelligent multi-agent cooperation in a high-dynamic environment of a soccer game with an orange golf ball on a green carpeted field [19].

The centralized position system provided by a camera pair mounted 6m above the field is a league particularity about the others. The shared vision system for the SSL, which is called SSL-Vision [26], processes images captured by the cameras. One of the objectives of the system proposal was to prevent each team from mounting its structure on the field. The system uses color segmentation, and the colored pattern detection above the robots showed good precision. However, the SSL-Vision cannot be considered a ground truth when used in a localization system, such as a Kalman filter for position estimation with the cameras providing measurements to correct the robots' location. Besides that, other sensors used in the SSL robot, like encoders attached to the wheels, cannot provide the position ground truth due to wheel slippage when accelerating, for example.

In real systems, such as mobile robots, determining the ground truth is nearly impossible. Except for certain specific cases and applications, the ground truth for positioning should be seen as a reliable approximation that is more accurate than other available options, rather than an exact representation of the robot's true position.

In this paper, we will present and evaluate the use of LiDARs to create a trustable and efficient ground truth system, especially for round robots, such as the ones used in the Small Size League of the RoboCup, shown in Fig. 1. Because of the high-dynamic environment that they are in, and the high precision needed in positioning to complete plays and score goals, there is a high need for ground truth since the camera

This study was financed in part by the Coordenação de Aperfeiçoamento de Pessoal de Nível Superior - Brasil (CAPES) - Finance Code 001

979-8-3315-5288-6/25/$31.00©2025 IEEE

system used in the league may have noise and struggle with light interference or overlap regions when using two or more cameras [1], [2], [7]. So, the camera system of the league can't be considered as ground truth, as the data provided from it may be being used in a positioning system, and internal sensors don't provide enough accuracy for it.

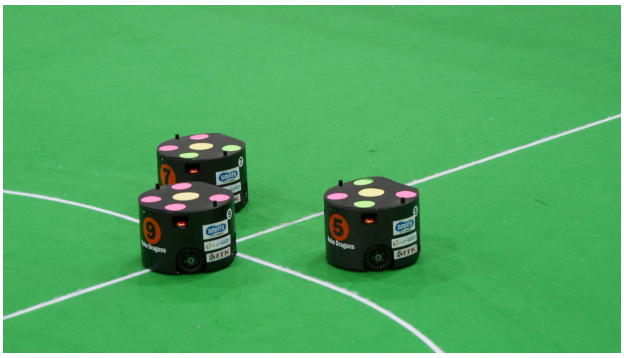

Fig. 1: Small Size League robot example.

Section II presents the related works about the ground truth theme in the RoboCup scene and other applications as well. Section III explains both the hardware architecture, i.e., the disposal of the lasers in the field test, and the software architecture, which contains the method applied to detect the robot's position and how the laser data is employed. Section IV describes the methodology used to analyze the system quality. Section V will present the results achieved by the tests. Finally, Section VI presents the conclusions of the comparison for position ground truth between the LiDARs system and the camera system used in the SSL.

II. Related works

The ground truth problem has been addressed through the years using different sensors and approaches [8], [11], [12], [17], [23]. Despite that, most parts of the ground truth systems use different types of cameras, and the smallest part of them use LiDARs but do not combine the data of multiple lasers.

[17] presents an approach applied to the Standard Platform League (SPL) from RoboCup. In this paper, the authors used four Kinects along the sidelines of the field to achieve a reliable ground truth for the humanoid robots of the league. The foreground mask extraction uses RGB and depth information in each frame. Then, using the created mask, the player's positions are obtained after a data fusion re-projects all the detected positions by the Kinects. The results were obtained by monitoring the position of the players using LiDAR, achieving a minimum error of 8mm and a maximum error of 476mm.

Following in the approaches used in the SPL, [8] also developed a system using a Kinect. The sensor driver from ROS provides the XYZ-RGB point cloud, which is applied Euclidean clustering to obtain one cluster per robot in the field, and then the position acquired is transformed to the global coordinates of the field. The authors obtained the results following the methodology described in this paper, i.e., placing the robot in known positions and capturing the system's output during 20 measurements. The authors achieved an average error of 10.41cm between the analyzed robot orientations.

[11] brings another approach developed especially for the SPL, but using one LiDAR to achieve the ground truth needed. In this case, the detection can be used for any object type, which is different from this paper, which leans into detecting particularly round robots. Besides that, the authors used only a laser for detection, but they commented that detecting points far from the laser position is challenging and the accuracy is worse. The authors suggest a multi-sensor approach to enhance the accuracy, which this paper tested since the detection uses two lasers on each field's half.

About examples out of the RoboCup field, [23] brings a low-cost distributed system of visual localization of mobile robots using cameras. The authors used six cameras above a polygon where the robot would traffic, and each camera zone is marked with Apriltag markers, and the robot is also marked with an Apriltag for its detection. The authors achieved an accuracy lower than 2cm in all the scenarios studied by changing the image resolution. Besides, the authors also analyzed the probability of detecting the robot marker, which depends on the marker size and the image resolution. The work differs from this paper in camera use since the capture of the polygon range uses six of it, besides adding an external marker in the robot for position detection by the system.

Finally, [12] presented a ground truth system developed especially for underwater benchmarking using a stereo camera pair and an external host computer for image processing and data recording. The paper compared two methods to detect the robot's position: template matching and color-based segmentation. The results showed a mean error higher than 2cm in all the axes (X, Y, and Z), besides the standard deviation, which is higher than 0.9cm. The paper differs from this on camera use, which leads to a high dependence on the environment illumination for better detection, which is an irrelevant problem when using LiDARs for detection.

III. Robot detection

A. Hardware architecture

The robot detection has been made using an RPLIDAR A1 [20] and an RPLIDAR S1 [22] in a test field of 4.5m long by 3.5m wide, each of them positioned in the center of a goal, as it can be seen in Fig. 2, where the A1 is placed on the left goal, while the S1 is on the right side.

The choice of this setting derives from initial tests made, besides the physical limitations of the lasers, since the sensors' maximum distance range is 6m [20]. So, if the sensors were placed on the field's corners, for example, the sensors could lose essential data depending on the robot's position. Each sensor was mounted on a base with a 5cm height to ensure that they could capture centralized data of the robot and avoid problems with distortions capturing the robot's wheels. However, since the objective is to evaluate positioning systems and there is no plan to be used directly in a game, it is admissible that the LiDARs can be placed further into the field

depending on the field size, the path planned for the tests, or the LiDAR used.

Compared to the traditional cameras setup used to detect the positions of the robots in the field in the SSL, this setup is easier to build, since it does not require the sensors to be placed in the ceiling and/or consirable height.

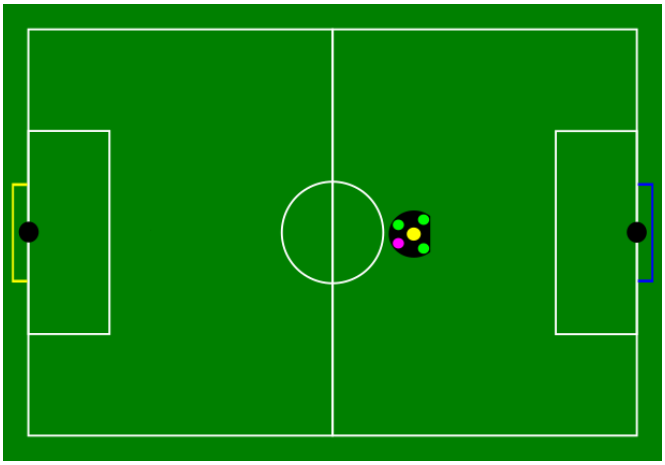

Fig. 2: Field test representation.

B. Software architecture

Fig. 3 shows the software architecture of the system proposed. That is based on a ROS2 package that will apply a scan matching to find the relative position between both lasers. After the system merges the data of both LiDARs in an image, different morphological operation process the image in order to improve the image quality, proceed with the image detection to recognize the circular shape on it, and then calculate the global coordinate of the robot, since the system calculates the position in the LiDAR frame in a first moment.

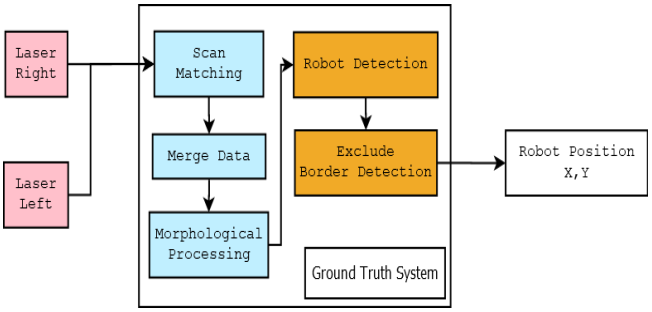

Fig. 3: Software architecture.

The first stage of the software is using scan matching made to find a transformation (translation, rotation, and scale) between both point clouds created by the lasers that fit better the data of both [15]. This stage is decisive since any centimeter difference between both data could lead to difficulty finding the robot's circular pattern or could add an offset in the position detected.

Basically, the scan matching works with two point clouds, the source P and the target S. The goal of the algorithm is to find a transformation $T = (R, t)$, composed by a rotation R and translation t, that minimizes the difference between both point clouds P and S, as described in (1), where r_i is the nearest point in the target point cloud S.

$$T^* = \arg\min \sum_{i=1}^{n} \|(Rp_i + t) - r_i\|^2 \tag{1}$$

So, the following stage of the software is merging the data of both LiDARs in an image mask, that will be called laser points image, by applying the transformation found in the scan matching stage. To obtain the sensors' data, SLAMTEC ROS2 Package [21] for the LiDAR A1 and S1 was used, given that it is an easier way to communicate with the sensors, initialize them, and receive the data. The ROS2 node publishes a laser scan message that contains the ranges captured by the sensor and their angles. With these data, it's possible to build the laser points image following (2), which shows how to determine the coordinates of each object detected in a scan, where r is the range in meters and θ is the respective angle to the range in radians.

$$\begin{cases} x = r * \cos(\theta) \\ y = r * \sin(\theta) \end{cases} \tag{2}$$

After merging the sensors' data, there is a layer to process the laser points image before recognizing the circular shape in the next stage. Morphological image processing is essential to refine the quality of images, reduce noise, and enhance the structural analysis, which leads to more accurate feature extraction on images [10]. First, the algorithm applies a subtle dilation to connect nearby points and then erodes them for better shape detection in the image. Finally, a delicate blur is applied to the laser points image for smoothness, thus reducing the noise in the image and the detection of false circles, as well as helping the pattern detection.

The next step of the software architecture is robot detection, that performs a circular or semi-circular detection in the laser points image. The method used for circular pattern detection is the Hough transform (HT). The technique was first created to detect lines in binary images, but other variations were suggested to detect different shapes, such as circular ones [13].

The circular HT relies on the circle equation demonstrated in (3), which the system calculates for each edge point in a pre-processed image according to the maximum and minimum limits for the radius. Each edge point contributes with votes for possible circles that can be part of. Thus, the votes are accumulated, and the local maxima provide the center locations and the radius of the circles in the images [6].

$$(x - a)^2 + (y - b)^2 = r^2 \tag{3}$$

In Fig. 4, it is possible to see two moments of the architecture. Fig. 4a shows the LiDARs' points after the scan matching and merge data stages, but before the morphological processing step, the blue points are from the right laser, and the green points are from the left laser. Fig. 4b shows the robot

detection step, where the Hough transform is applied to the laser points image to detect a circular pattern.

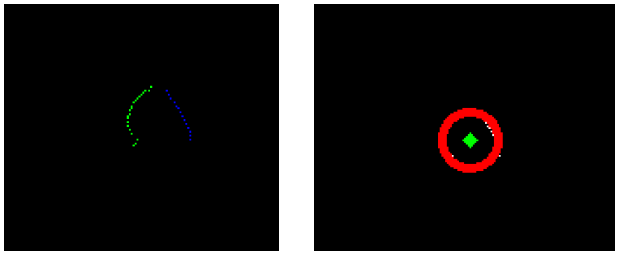

(a) Raw image of the LiDARs points.

(b) Circle detected by the system.

Fig. 4: Two steps of the software architecture.

A last step of post processing is done to detect and exclude false positives detected in the field borders since most parts of the points detected by the laser are concentrated on field boundaries. Basically, the frontier coordinates are excluded and the detection is focused within the field.

IV. Methodology

This section explains the tests used to evaluate the system, the robot used during the tests, and the metrics analyzed to proof the ground truth system proposed in this paper.

As described previously, the robot used in the tests is one used in official matches of the SSL, so it fits in a 180x150mm cylinder, but it is linearly cut off on the front side to allocate the robot's dribbler system to control the ball in the game. Besides, the field used for the tests is 4.5x3.5m.

The vision system used in the tests is composed by two different cameras, each one positioned in each field's half. The cameras used are listed below. The first is placed on the right half of the field and the second is positioned on the left.

- Logitech BRIO 4K UHD [9]
- Stingray F046C [24] + Tamron 12VM412ASIR Lens

For the LiDARs system an RPLIDAR A1 [20] and an RPLIDAR S1 [22] were used in this paper, both of which are low-cost 360-degree LiDARs. The first uses the laser triangulation ranging principle [4] to achieve the data, while the second is based on the time-of-flight technology [25]. Both were operating with a scan frequency of 10Hz, and the A1 was used in Boost scan mode (787 points captured), while the S1 was in DenseBoost scan mode (925 points captured).

The notebook used to perform the robot detection in the laser points image has the following specifications:

- Intel i7-7700HQ CPU @ 2.80GHz
- NVIDIA Geforce MX150
- 16GB RAM
- Ubuntu 22.04.5 LTS x86_64

In order to evaluate the proposed ground truth system using LiDARs, the robot will be placed in 17 known positions in the field, while the position is obtained by the LiDARs system and the vision system of the league. Both systems will be compared with the real coordinate, taken using a measuring tape to obtain a better precision.

For each position the LiDARs system output will be recorded for 200 detections, while the data provided by the vision system is also being recorded. Then, the mean of these samples will be taken and compared with the known position to calculate the error, as well as their standard deviation will also be calculated in order to analyze the system stability.

The 17 scenarios are divided into two sets. First, the scenarios placed more centralized with the field coordinates (4-6, 8-10, 12-14) and the points disposed far from the field center (1-3, 7, 11, 15-17). The scenarios can be seen in Fig. 5, represented by the red circles, while the blue circles represent the cameras' positions, and the black circles the LiDARs' positions. The centralized scenarios will handle how the LiDAR system deals with equidistant points between both lasers. The dispersed scenarios will be of use to observe how the system deals with points near one laser than the other and in scenarios near the field boundaries.

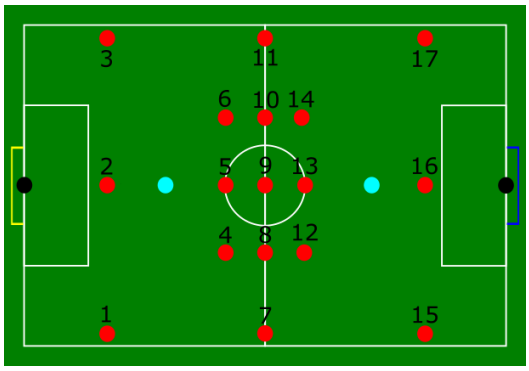

Fig. 5: Positions of the tests.

Besides that, since two cameras are placed for the vision system, the scenarios will be divided into three sets. That will help to see the differences between the captures made by each and observe how they work in the overlap region located along the middle of the field. The sets will be called Quadrant. The first deals with scenarios 1-6, since only the left camera captures these scenarios, and the second deals with scenarios 7-14, which are the scenarios positioned on the overlap of both cameras, and the third deals with scenarios 15-17, the scenarios captured only by the right camera. These sets will show how the SSL-Vision deals with distortion caused by the fish eye effect, mainly on the borders of the image captured by them. It's supposed a substantial error in the output coordinates of the SSL-Vision when they are far from the camera's center.

V. Results

Tables I and II summarize the results achieved by the laser and vision for the X and Y axes, respectively, in the 17 scenarios. The Real column indicates the known coordinates of the robot's position, and the Laser and Vision columns show the mean and standard deviation of the samples measured for

TABLE I: Results achieved for the X axis in the SSL field.

Scenario	Real [cm]	Laser [cm]	Vision [cm]
1	-91,5	-91.797 +- 0.584	-92.945 +- 0.026
2	-88,1	-87.594 +- 0.437	-89.099 +- 0.023
3	-93	-92.510 +- 0.391	-93.397 +- 0.049
4	-55	-54.584 +- 0.703	-55.389 +- 0.037
5	-51	-50.321 +- 0.655	-51.323 +- 0.017
6	-54,5	-54.504 +- 0.926	-55.363 +- 0.037
7	0	1.092 +- 0.674	0.488 +- 0.012
8	0	0.390 +- 0.624	0.370 +- 0.073
9	0	0.552 +- 0.513	-0.158 +- 0.061
10	0	0.786 +- 0.478	-0.505 +- 0.036
11	0	0.972 +- 0.953	0.178 +- 0.025
12	61,3	61.859 +- 0.649	61.588 +- 0.017
13	52	51.964 +- 0.519	52.379 +- 0.011
14	53	53.742 +- 1.036	52.868 +- 0.046
15	101	101.653 +- 1.450	100.866 +- 0.015
16	99	99.683 +- 0.554	98.785 +- 0.017
17	97	97.526 +- 1.509	96.679 +- 0.018

TABLE II: Results achieved for the Y axis in the SSL field.

Scenario	Real [cm]	Laser [cm]	Vision [cm]
1	-138,5	-137.784 +- 0.726	-139.464 +- 0.047
2	0	0.844 +- 1.475	0.365 +- 0.018
3	132	131.688 +- 0.625	134.255 +- 0.022
4	-85	-84.104 +- 0.851	-85.172 +- 0.016
5	0	-0.518 +- 1.424	0.690 +- 0.036
6	81,5	80.801 +- 1.435	83.025 +- 0.018
7	-141	-140.488 +- 0.742	-139.829 +- 0.014
8	-82,5	-82.172 +- 0.978	-82.306 +- 0.061
9	0	0.668 +- 1.052	0.963 +- 0.041
10	83,5	84.431 +- 1.781	85.154 +- 0.028
11	125,5	125.017 +- 0.925	126.895 +- 0.083
12	-92,3	-92.848 +- 0.900	-91.665 +- 0.015
13	0	-0.568 +- 0.879	0.810 +- 0.014
14	85,3	85.046 +- 1.317	86.171 +- 0.053
15	-135,5	-135.906 +- 0.813	-135.158 +- 0.022
16	0	0.048 +- 0.598	1.236 +- 0.016
17	123,5	123.125 +- 1.015	124.690 +- 0.023

each system. All the measurements in these and the following tables are in centimeters.

Table III shows the mean error and standard deviation of all the scenarios, the centralized and dispersed sets of points, in the X and Y axes. It is possible to analyze that the mean error for the X-axis of both systems is comparable, with a difference of almost 0.1cm between them. For the Y axis in all scenarios, it's possible to see a considerable difference between them, near 0.43cm. This difference can be explained by the distortion occurring in the borders of the cameras' image, increasing the error in these points since they have a distance greater from the cameras on the Y-axis than the X-axis.

TABLE III: Scenarios mean error and standard deviation.

	X - Laser	X - Vision	Y - Laser	Y - Vision
Mean error	0,5519	0,4461	0,5356	0,9665
Error - Centralized	0,4626	0,3785	0,6011	0,8348
Error - Dispersed	0,6523	0,5221	0,4620	1,1147
Mean Std. Dev.	0,7444	0,0305	1,0315	0,0310
Std. Dev. - Centralized	0,6781	0,0372	1,1796	0,0313
Std. Dev. - Dispersed	0,8190	0,0231	0,8648	0,0306

The errors between the centralized and dispersed sets show that the camera system deals better with the positions in the center of the field, which the distortion on the borders of the cameras' image can explain. That effect cannot be seen when analyzing the LiDAR system, showing that the detection made by it is regular in all parts of the fields, and also proving the advantages of using two LiDARs to enhance the detection of the circular pattern in the field.

Analyzing the standard deviation metric in Table III, it is possible to notice that the camera system of the SSL is much better than the LiDARs system since the detection was almost 0,3mm dispersed from the mean when observing all scenarios in X, and less than 0,4mm and 0,3mm for the centralized and dispersed scenarios, respectively. For the Y-axis, the results were practically the same. Compared with the LiDAR system, this was worse, but the results are still acceptable, and the laser points image resolution used to perform the pattern detection can explain it. The laser points image was 1000x1000 pixels, each of them means 0.533cm in the real world because of the scale. Thus, the minor difference in the detection leads to a half-centimeter difference in the robot position.

Analyzing the quadrants, Tables IV and V show the results summarized for them in the X and Y axes. Notably, the quadrant of the left camera is worse for the X-axis when analyzing the mean error, with more than double the error when compared with quadrants 2 and 3. Using a fish eye lens in the left camera can explain this effect since it leads to considerable distortion compared to the right camera. For the Y-axis in all quadrants, it is possible to see that the mean error is worse compared with the LiDAR system at least 50%.

TABLE IV: Results for the quadrants in X axis.

	Error X - Laser	**Error X - Vis.**	**Std. Dev. X - Laser**	**Std. Dev. X - Vis.**
Quad. 1	0,3986	0,7360	0,6224	0,0315
Quad. 2	0,6411	0,3122	0,6807	0,0351
Quad. 3	0,6206	0,2233	1,1710	0,01667

TABLE V: Results for the quadrants in Y axis.

	Error Y - Laser	**Error Y - Vis.**	**Std. Dev. Y - Laser**	**Std. Dev. Y - Vis.**
Quad. 1	0,6641	0,9951	1,0893	0,0261
Quad. 2	0,5844	1,0754	1,0956	0,0454
Quad. 3	0,3665	0,8473	0,9203	0,0238

Analyzing the standard deviation, it's not noticeable any influence of the camera's positioning on both axes. Besides, the camera system is still better than the LiDAR system in all quadrants for both axes. When evaluating the LiDARs system for both axes, it is not possible to notice a significant difference between the quadrants, showing that the detection made by the lasers is regular, and the errors accumulated in long distances for one laser are compensated by the other laser.

VI. Conclusion

This work presents an approach for position ground truth using two LiDARs, especially for round robots. The system is compared with the camera system of the Small Size League from RoboCup. Ground truth is needed when developing a localization system since evaluating the estimated position with the robot's actual localization in the real world is crucial. Besides, reliable ground truth works alongside a localization system for calibrating it, like a sensor fusion for indoor environments, odometry adjustment, or camera calibration.

According to the results presented previously in Section V, the developed ground truth system had good results in the mean error calculated between the system output and the accurate coordinates measured using a measuring tape. In both axes, the mean error achieved for the developed system was almost 0.5cm, which is better than the camera system on the Y axis (an error of approximately 0.96cm) and about 0.1cm worse on the X axis. These comparisons are also noticeable when analyzing the centralized and dispersed scenarios.

When analyzing the standard deviation, it is possible to notice that the camera system is much better than the LiDARs system since the standard deviation of the second one is 0.74cm and 1.03cm for the X and Y axes, respectively, while for the vision system, it is near 0.03cm for both axes. These insights are noticeable when analyzing the centralized and dispersed scenarios. The scale and image resolution (1000x1000 pixels) used for the LiDAR system can explain these results.

When analyzing the quadrants described, it is possible to confirm that the vision system was worse when comparing the LiDAR system on the Y-axis. For the X-axis, it is noticeable that one of the cameras used distorted the correct position of the robot because of the use of a lens in it. The standard deviation of each quadrant followed the insights observed in the mean of all scenarios, which is the vision system being much superior compared with the laser system.

In conclusion, the LiDARs system developed can be used as a position ground truth system for round robots since the mean error and mean standard deviation results presented are not notable, practically less than 1 centimeter on both. Besides, the results could be enhanced using more powerful LiDARs that provide more points and better precision over the distance. Besides, the LiDAR scan frequency of 10Hz is a bottleneck since it limits the system detection frequency. The detection can occur for any diameter, depending on the scale used in positioning the laser data in the laser points image.

Future works could include adding a Kalman filter to have a smooth system and decrease the possible variations in the detection. Besides, using a more powerful notebook aims to increase the LiDAR system image resolution, which should provide a better standard deviation to the system. Moreover, adding at least one more LiDAR can increase the system's accuracy, thus achieving results even closer to the ground truth, and it can be possible to determine the robot's orientation by detecting the robot's dribbler system.

ACKNOWLEDGEMENTS

The authors would like to thank the University Center of FEI, the RoboFEI team and CAPES for their support.

REFERENCES

[1] Aoki, S., Degawa, T., Fujihara, K., Notsu, Y., Beppu, T.: Mct susano logics 2016 team description. Available for download in http://wiki. robocup. org/images/2/27/Small Size League-RoboCup (2016)

[2] Beppu, T., Aoki, S., Horiuchi, T.: A shared multi-particle filter for ball position estimation in robocup small size league soccer games. In: 2016 International Conference on Autonomous Robot Systems and Competitions (ICARSC). pp. 311–316 (2016). https://doi.org/10.1109/ICARSC.2016.24

[3] Chen, W., Xu, J., Zhao, X., Liu, Y., Yang, J.: Separated sonar localization system for indoor robot navigation. IEEE Transactions on Industrial Electronics **68**(7), 6042–6052 (2021). https://doi.org/10.1109/TIE.2020.2994856

[4] English, C., Zhu, S., Smith, C., Ruel, S., Christie, I.: Tridar: A hybrid sensor for exploiting the complimentary nature of triangulation and lidar technologies. In: Proceedings of the 8th International Symposium on Artificial Intelligence, Robotics and Automation in Space. vol. 1 (2005)

[5] Guan, W., Chen, S., Wen, S., Tan, Z., Song, H., Hou, W.: High-accuracy robot indoor localization scheme based on robot operating system using visible light positioning. IEEE Photonics Journal **12**(2), 1–16 (2020). https://doi.org/10.1109/JPHOT.2020.2981485

[6] Hassanein, A.S., Mohammad, S., Sameer, M., Ragab, M.E.: A survey on hough transform, theory, techniques and applications. arXiv preprint arXiv:1502.02160 (2015)

[7] Huang, Z., Chen, L., Li, J., Wang, Y., Chen, Z., Wen, L., Gu, J., Hu, P., Xiong, R.: Zjunlict extended team description paper for robocup 2019. RoboCup (2019)

[8] Khandelwal, P., Stone, P.: A low cost ground truth detection system for robocup using the kinect. In: RoboCup 2011: Robot Soccer World Cup XV 15. pp. 515–527. Springer (2012)

[9] Logitech: BRIO ULTRA HD BUSINESS WEBCAM (3 2021)

[10] Lotufo, R.A., Audigier, R., Saúde, A.V., Machado, R.C.: Morphological image processing. In: Microscope image processing, pp. 75–117. Elsevier (2023)

[11] Marchant, R., Guerrero, P., Ruiz-del Solar, J.: A portable ground-truth system based on a laser sensor. In: RoboCup 2011: Robot Soccer World Cup XV 15. pp. 234–245. Springer (2012)

[12] Martins, A., Dias, A., Silva, H., Almeida, J., Gonçalves, P., Lopes, F., Faria, A., Ribeiro, J., Silva, E.: Groundtruth system for underwater benchmarking. In: 2013 OCEANS - San Diego. pp. 1–5 (2013). https://doi.org/10.23919/OCEANS.2013.6741307

[13] Mukhopadhyay, P., Chaudhuri, B.B.: A survey of hough transform. Pattern Recognition **48**(3), 993–1010 (2015)

[14] Niemüller, T., Ferrein, A., Eckel, G., Pirro, D., Podbregar, P., Kellner, T., Rath, C., Steinbauer, G.: Providing ground-truth data for the nao robot platform. In: RoboCup 2010: Robot Soccer World Cup XIV 14. pp. 133–144. Springer (2011)

[15] Nieto, J., Bailey, T., Nebot, E.: Recursive scan-matching slam. Robotics and Autonomous Systems **55**(1), 39–49 (2007). https://doi.org/https://doi.org/10.1016/j.robot.2006.06.008, https://www.sciencedirect.com/science/article/pii/S0921889006001461, simultaneous Localisation and Map Building

[16] Panigrahi, P.K., Bisoy, S.K.: Localization strategies for autonomous mobile robots: A review. Journal of King Saud University - Computer and Information Sciences **34**(8, Part B), 6019–6039 (2022). https://doi.org/https://doi.org/10.1016/j.jksuci.2021.02.015, https://www.sciencedirect.com/science/article/pii/S1319157821000550

[17] Pennisi, A., Bloisi, D.D., Iocchi, L., Nardi, D.: Ground truth acquisition of humanoid soccer robot behaviour. In: Behnke, S., Veloso, M., Visser, A., Xiong, R. (eds.) RoboCup 2013: Robot World Cup XVII. pp. 560–567. Springer Berlin Heidelberg, Berlin, Heidelberg (2014)

[18] RoboCup: Robocup objective (9 2019), https://ssl.robocup.org/rules/, access in 23 dec. 2024 at 21:33

[19] RoboCup-SSL: Small size league rules (5 2024), https://ssl.robocup.org/rules/, access in 23 dec. 2024 at 21:33

[20] SLAMTEC: RPLIDAR A1 - Low Cost Degree Laser Range Scanner (7 2016), rev. 10

[21] SLAMTEC: Slamtec lidar ros2 package. https://github.com/Slamtec/rplidar_ros/tree/ros2 (2016)

[22] SLAMTEC: RPLIDAR S1 - Low Cost Degree Laser Range Scanner (1 2018), rev. 10

[23] Sorokumov, S., Glazunov, S., Chaika, K.: Distributed visual-based ground truth system for mobile robotics

[24] Technologies, A.V.: Technical Manual (4 2011), v4.4.2

[25] Yang, T., Li, Y., Zhao, C., Yao, D., Chen, G., Sun, L., Krajnik, T., Yan, Z.: 3d tof lidar in mobile robotics: A review. arXiv preprint arXiv:2202.11025 (2022)

[26] Zickler, S., Laue, T., Birbach, O., Wongphati, M., Veloso, M.: Ssl-vision: The shared vision system for the robocup small size league. In: Baltes, J., Lagoudakis, M.G., Naruse, T., Ghidary, S.S. (eds.) RoboCup 2009: Robot Soccer World Cup XIII. pp. 425–436. Springer Berlin Heidelberg, Berlin, Heidelberg (2010)